LAWRENCE
LIVERMORE
NATIONAL
LABORATORY

LLNL-PROC-758642

SIMULATION OF CROSS-SEPARATRIX EDGE PLASMA TRANSPORT WITH THE CONTINUUM GYROKINETIC CODE COGENT

M. Dorf, M. Dorr, D. Ghosh, J. Hittinger, M. Umansky, J. Angus, A. Pankin

September 21, 2018

27th IAEA Fusion Energy Conference (FEC 2018)
Gandhinagar, India
October 22, 2018 through October 27, 2018

Disclaimer

SIMULATION OF CROSS-SEPARATRIX EDGE PLASMA TRANSPORT WITH THE CONTINUUM GYROKINETIC CODE COGENT

M. DORF, M. DORR, D. GHOSH, J. HITTINGER, M. UMANSKY, J. ANGUS
Lawrence Livermore National Laboratory
Livermore, California 94550, USA
Email: dorf1@llnl.gov

A. PANKIN
Tech-X Corporation,
Boulder, Colorado 80303, USA

Abstract

Axisymmetric (4D) simulations using the finite-volume code COGENT are performed to explore the role of ion kinetic effects in tokamak edge plasmas. The simulation model solves the long wavelength limit of the full-F gyrokinetic equation for ion species coupled to the 2D quasi-neutrality equation for electrostatic potential variations, where a fluid model is used for an electron response. The ion-ion collisions are described by the nonlinear Fokker-Plank operator and the effects of anomalous transport are included via a radial diffusion model. Illustrative simulations are performed for the parameters characteristic of the LTX tokamak. The development of 5D COGENT for edge plasma turbulence modelling is also reported. To that end, the slab-geometry 5D version has been developed and successfully verified in simulations of the collisionless drift-wave instability that involve gyrokinetic equations for both ion and electron species coupled to the long-wavelength limit of the 3D gyro-Poisson equation. Recent work is focused on extending the 5D code to include the effects of a tokamak edge magnetic geometry.

1. INTRODUCTION

Development of full-F computational methods for kinetic plasma transport modeling becomes increasingly important in a tokamak edge region where an ion distribution can substantially deviate from a local Maxwellian distribution and therefore a so-called delta-F approximation becomes invalid. Presently, there are two main approaches to solving a kinetic equation (a) the particle in cell (PIC) method, in which macroparticles are used to represent a distribution function, and (b) the continuum (Eulerian) approach, in which a distribution function is represented on a phase-space grid. While the PIC methods can easily handle a complex magnetic geometry of a tokamak edge region [1], modeling of low-amplitude edge turbulence subject to an adequate representation of a background quasi-equilibrium dynamics may require a very large number of macroparticles to suppress statistical errors in full-F PIC simulations. Therefore, it is of importance to develop continuum (Eulerian) discretization schemes for edge plasma modeling.

This paper presents the progress with the continuum high-order finite-volume gyrokinetic code COGENT for edge plasma modeling [2]. The code is unique in that it is based on a consistent high-order discretization and interpolation of the underlying equations, and hence the error (in particular near the X-point) can be bounded. It utilizes multiblock grid technology, in which logically distinct blocks are smoothly mapped from rectangular computational domains and a high-order interpolation is used to provide data communication between the blocks. The code presently solves the gyrokinetic system in the long-wavelength limit, i.e., assuming $k_\perp \rho_i \ll 1$. Here, ρ_i is the ion gyroradius and $k_\perp$ is the characteristic wavelength for electrostatic potential variations. Multi-species gyrokinetic equations can be solved with a number of increasingly detailed collision models including the nonlinear Fokker-Plank operator [3]. Options for self-consistent electrostatic potential perturbations include the gyro-Poisson equation, which supports kinetic electrons [4], and the quasi-neutrality equation, $\boldsymbol{\nabla} \cdot \boldsymbol{j} = 0$, which can be coupled to a fluid electron model [2]. Progress with the COGENT code is concurrently being made in two directions: (i) 4D axisymmetric modeling of cross-separatrix edge plasma transport (Sec. 2) and (ii) moving toward a full 5D edge turbulence code capability (Sec. 3).

2. 4D AXISYMMETIC MODELING OF CROSS-SEPARATRIX EDGE PLASMA TRANSPORT

The code solves the long-wavelength limit of the gyrokinetic equation for a gyroaveraged distribution function $f_\alpha(\boldsymbol{R}, v_\parallel, \mu)$, written in a conservative form:

$$\frac{\partial B^*_{\|\alpha} f_\alpha}{\partial t} + \nabla_{\mathbf{R}} \cdot \left(\dot{\mathbf{R}}_\alpha B^*_{\|\alpha} f_\alpha\right) + \frac{\partial}{\partial \mathrm{v}_\|}\left(\dot{\mathrm{v}}_\| B^*_{\|\alpha} f_\alpha\right) = C_\alpha[B^*_{\|\alpha} f_\alpha] + T^{AN}_\alpha[B^*_{\|\alpha} f_\alpha]. \quad (1)$$

Here, α denotes the particle species, $\mathbf{R}$ is the gyrocenter coordinate, $\nabla_{\mathbf{R}}$ is the gradient with respect to $\mathbf{R}$, and the phase-space guiding-center velocities are given by

$$\dot{\mathbf{R}}_\alpha = \frac{1}{B^*_{\|\alpha}}\left[\mathrm{v}_\| \mathbf{B}^*_\alpha + \frac{1}{Z_\alpha e}\mathbf{b} \times (Z_\alpha e \nabla\Phi + \mu \nabla B)\right], \quad (2)$$

$$\dot{\mathrm{v}}_{\|\alpha} = -\frac{1}{m_\alpha B^*_{\|\alpha}} \mathbf{B}^*_\alpha \cdot (Z_\alpha e \nabla\Phi + \mu \nabla B), \quad (3)$$

where m_α and Z_α are the species mass and charge state, respectively, e is the electron charge, $\mathbf{B}(\mathbf{R}) = B\mathbf{b}$ is the magnetic field with $\mathbf{b}$ denoting the unit vector along the field, $\mathbf{B}^*_\alpha(\mathbf{R}, \mathrm{v}_\|) \equiv \mathbf{B} + (m_\alpha \mathrm{v}_\| / Z_\alpha e)\nabla \times \mathbf{b}$, $B^*_{\|\alpha}(\mathbf{R}, \mathrm{v}_\|) \equiv \mathbf{B}^*_\alpha \cdot \mathbf{b}$. The left-hand-side of Eq. (1) represents the gyrokinetic Vlasov equation, C_α is the collisional operator, and T^{AN}_α is the anomalous transport model operator used to mimic the effects of turbulence-driven transport [2]. Axisymmetric 4D modelling assumes the distribution function in Eq. (1) to be independent of the toroidal angle.

Numerical algorithms implemented in COGENT enable solving Eq. (1) for evolution of a gyro-averaged distribution function on arbitrary spatial grids represented by logically distinct blocks that are smoothly mapped from rectangular computational domains. The available geometry choices include slab, cylindrical, and Miller single-block options as well as a single-null multiblock geometry. Strong anisotropy of plasma transport motivates the use of coordinate surfaces, which are aligned with isosurfaces of the magnetic flux function, however the presence of an X-point where metric coefficients diverge requires smoothing of the coordinate surfaces in each block (by de-aligning) in the X-point vicinity in order to achieve high-order convergence.

Recently 4th-order convergence of the gyrokinetic Vlasov model [i.e., LHS of Eq. (1)] involving a single ion species and a prescribed (fixed) electrostatic potential has been reported for the case of a single-null geometry [5]. While this proof-of-principle result is of great importance, more advanced simulation involving fluid electrons and 2D self-consistent potential demonstrated that even a modest level of grid de-alignment near the X-point, which was sufficient to achieve convergence in the aforementioned simulations involving only ion transport [5], was no longer sufficient and provided strong numerical pollution once the effects of electron dynamics and self-consistent electric fields are included [2]. Self-consistent 2D potential variations Φ are included in COGENT simulations of the 4D cross-separatrix transport by making use of the following quasi-neutrality model [2]:

$$\nabla_\perp \cdot \left(\frac{e^2 n_i}{m_i \Omega_i^2} \nabla_\perp \frac{\partial \Phi}{\partial t}\right) = \nabla_\perp \cdot \boldsymbol{j}_{i,\perp} + \nabla_\| \left[\sigma_\| \left(\frac{1}{e n_i}\nabla_\| P_e - \nabla_\| \Phi + \frac{0.71}{e}\nabla_\| T_e\right)\right] - \nabla_\perp \cdot \left(\frac{c^2 m_i n_i \nu_{cx}}{B^2}\nabla_\perp \Phi\right). \quad (4)$$

Here, the LHS of Eq. (4) corresponds to the divergence of the polarization current, and the terms on the RHS correspond to the divergences of the perpendicular ion guiding-center current $\boldsymbol{j}_{\perp,i} = \int \dot{\boldsymbol{R}}_{i,\perp} f_i B^*_{\|,i} dv_\| d\mu$, the parallel plasma current, $j_\|$, and the perpendicular current driven by charge-exchange collisions with neutrals, respectively. Note that the model does not include the perpendicular electron current and contains the contribution from the $E \times B$ drift in the ion perpendicular current. Although such formulation may seem somewhat different from what is typically used in fluid codes [6-7], Eq. (4) can still adequately describe self-consistent potential variations. Indeed, due to a large value of the electron parallel conductivity, $\sigma_\|$, the potential distribution on open field lines and its poloidal variations on closed field lines are set by $j_\| \approx 0$. The remaining unknown field quantity – the radial electric field in a closed-field-line core region – is described by the flux-surface average of Eq. (4), which only neglects a small $O\left(\sqrt{m_e/m_i}\right)$ contribution from the flux-surface-averaged radial electron current. The presence of a large parallel electron conductivity in Eq. (4) requires a flux-aligned grid in order to avoid numerical pollution, and the conditions on the level of grid dealignment in a vicinity of the X-point are found to be more severe than those for the problems involving ion transport only. Furthermore, fast times scales associated with high electron parallel conductivity yield a very tight Courant condition for explicit time integration, and therefore Eq. (4) is treated implicitly.

Equation (4) for self-consistent potential variations involves an electron temperature and neutral density (via the charge-exchange collision frequency, ν_{cx}), and therefore should be coupled to a model for electron and neutral transport. Fully kinetic description of electron and neutral species yields substantial numerical challenges due to the presence of fast time scales, namely the parallel electron transport scale $\tau_e \sim L_\| / V_{Te}$ and the perpendicular

neutral transport scale, $\tau_g \sim L_\perp / V_{Ti}$. Here, $L_\parallel$ and $L_\perp$ are the length scales for parallel and perpendicular variations in plasma profiles, and V_{Te} and V_{Ti} denote the electron and ion thermal velocity, respectively. A simpler approach to including the effects of electrons and neutrals is to make use of fluid models. To that end the code has been extended to support time integration of an arbitrary number of fluid equations together with gyrokinetic equations. Furthermore, to facilitate time integration an IMEX (Implicit-Explicit) time integration capability has been developed such that selected stiff-terms (e.g., diffusion-like) can be advanced implicitly [8]. The IMEX scheme is general and can be applied to any terms in the kinetic or fluid equations, however its efficiency depends on availability of the corresponding preconditioners. While development of detailed electron and neutral fluid models is underway, it is possible to obtain a solution to Eqs. (1)-(4) by making use of prescribed (fixed) profiles for the electron temperature and neutral density. For instance, such profiles can be adopted from transport solutions obtained by fluid codes like SOLPS [6] or UEDGE [7]. Obtaining COGENT transport solutions informed by a fluid-code solution for electrons and neutrals, can be particularly important for clarifying the role of ion kinetic effects.

Recently, the first continuum kinetic calculation with the 4D COGENT code adopting a simple (isothermal) model for electrons and an ad-hoc model for neutral density was performed for parameters characteristic of the DIII-D tokamak [2]. The simulations demonstrated the values of intrinsic rotation and radial electric field qualitatively similar to those observed in DIII-D experiments. Here, we present the results of illustrative simulations for the parameters characteristic of the Lithium Tokamak Experiment (LTX) experiment [9]. The distinguishing feature of the LTX facility is the use of Lithium wall-coatings that reduce recycling and minimize neutral gas content. Reduced interaction with cold neutral gas particles leads to mitigation of plasma cooling in a scrape-off-layer (SOL) region, such that the value of a SOL plasma temperature becomes comparable to its hot-core counterpart. This, in turn, emphasizes the role of ion kinetic effects in the SOL region as collisionality rapidly decreases with an increase in the plasma temperature. Low-collisionallity of the SOL region together with the pronounced magnetic bottle effect of a spherical tokamak geometry make edge kinetic solutions for LTX to be qualitatively different from those realized on the DIII-D facility. In particular, much stronger deviation from a Maxwellian distribution and more pronounced poloidal variations in the electrostatic potential have been observed in the COGNET LTX-like simulations as compared to the results of the COGENT DIII-D modelling reported in Ref. [2].

The results of illustrative COGENT simulations for the LTX-like parameters are shown in Figs. 1-2. The simulation model is described in detail in Ref. [2], and here we only comment on the specific parameters used for the calculations presented in this section. An ad-hoc analytic magnetic geometry is adopted such that its critical parameters including major and minor radii, and the magnetic bottle ratio are chosen to be roughly consistent with the LTX geometry. The toroidal magnetic field is determined from $B_\phi R = 0.08\ \mathrm{T}\cdot\mathrm{m}$, where R is the major radius coordinate, and the ratio of the toroidal to poloidal magnetic field at the outer midplane is $B_\phi / B_\theta \sim 3$. A single-species hydrogen plasma is considered. Weak ion-ion collisions, $R_0 / V_{Ti}\tau_i \sim 0.01$, are described with the nonlinear Fokker-Plank operator [3], and a simple radial diffusion model [2] with the uniform diffusion coefficient $D = 4.1\ \mathrm{m/s^2}$ is adopted for anomalous transport. Here, R_0 is a tokamak major radius and τ_i is Braginskii's collisional time for the ion species. A Maxwellian distribution function with fixed values of the density, $n_0 = 2.5 \times 10^{18}\ \mathrm{m^{-3}}$, and temperature, $T_0 = 70$ eV, is assumed at the inner core boundary. Absorbing, i.e., zero in-flux, boundary condition is imposed at the diverter plates boundaries, and the zero Neuman boundary condition, i.e., $\partial f_i / \partial \psi = 0$ is used at the SOL and private flux (PF) domain boundaries. The boundary conditions for the potential distribution include the zero Dirichlet conditions at the diverter plates, the zero Neumann conditions at the SOL and PF boundaries, and a flux-surface averaged quasineutrality condition at the inner core boundary [2]. The electron temperature in Eq. (4) is taken to be uniform $T_e = T_0 = 70$ eV, and the corresponding uniform value of $\sigma_\parallel = 7.2 \times 10^{15}\mathrm{s^{-1}}$ is used for parallel conductivity. It is instructive to comment on the validity of the electron fluid model adopted here primarily for simplicity reasons. The weakly-collisional SOL plasma is confined by the magnetic-bottle effect with a confinement time determined by the ion-ion collisional scattering into the loss-cone region [see Fig. 2]. The electrons are confined by the build-up of the electrostatic potential [see Fig. 1] and have sufficient time to relax (due to rapid electron-electron collisions) to a locally Maxwellian distribution, which is consistent with a fluid description. The neutral gas effects are presently included in the simulation model only via the last term on the RHS of Eq. (4). As the LTX facility targets a low content of a neutral gas, the charge-exchange collision frequency, ν_{cx}, is set to zero everywhere except a narrow layer around the separatrix, where the charge-exchange perpendicular current term is used to provide smoothing of a sharp transition layer in the radial electric field profile [2].

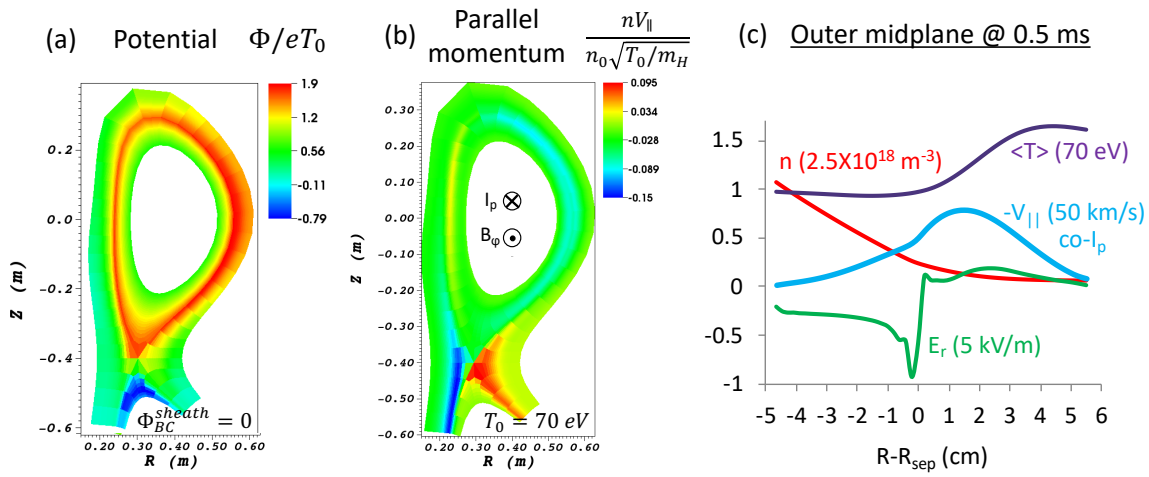

FIG. 1. Results of the illustrative 4D COGENT simulations of cross-separatrix axisymmetric transport for the parameters characteristic of the LTX experiment. Note substantial poloidal variations of electrostatic potential in the SOL region [Frame (a)], which are consistent with the magnetic bottle confinement and plasma density increase at the outer midplane. The average temperature $\langle T \rangle$ shown in purple in Frame (c) is computed as the total second moment of the ion distribution function. The grid resolution is specified by $(N_\psi = 24, N_\theta = 32), (N_\psi = 24, N_\theta = 40)$, and $(N_\psi = 8, N_\theta = 8)$, in the core, SOL, and private-flux regions, respectively, and the velocity grid is given by $(N_{v_\parallel} = 96, N_\mu = 96)$. Here, N_ψ, N_θ, $N_{v_\parallel}$, and N_μ corresponds to the number of cells in the directions of the radial coordinate, poloidal coordinate, parallel velocity, and magnetic moment, respectively.

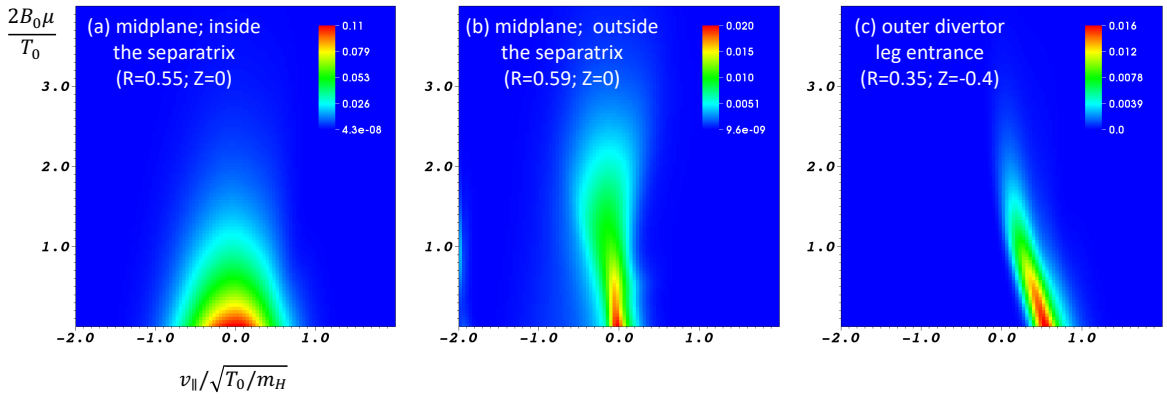

FIG. 2. Normalized hydrogen distribution function plotted at the midplane (a) 2 cm inside and (b) 2 cm outside of the separatrix, and (c) at the entrance to the outer divertor leg region. Note substantial deviation from a Maxwellian distribution in the outer SOL region and a pronounced magnetic bottle effect that confines ions with large values of a perpendicular energy (see Frame b).

3. MOVING TOWARD 5D EDGE TURBULENCE CODE

Rapid progress is concurrently being made toward development of a 5D code for edge turbulence modeling. As a first step, a single-block slab version describing evolution of a 5D gyroaveraged distribution function $f(x, y, z, v_{\|}, \mu)$ in the Cartesian coordinate system has been implemented. This version has been successfully verified in the simulations of the collisionless (universal) drift-wave instability, which employed gyrokinetic equations for the electron and ion species coupled to the long-wavelength limit of the gyroPoisson equation [4]. More recent work is focused on the development of a finite-volume code that can handle a diverter tokamak geometry. Short-wavelength turbulence that determines transport properties of a tokamak plasma is distinguished by highly-anisotropic perturbations, which are aligned with the magnetic field, and therefore motivate the use of a field-aligned coordinate system. However, the presence of the X-point and a strong magnetic shear in the edge of a diverted tokamak generates significant distortion of the controlled volumes if a globally field-aligned coordinate system is used. To deal with this issue, the following discretization concept has been adopted (see Fig. 3). The toroidal direction is divided into a number of blocks (wedges) such that a local coordinate system is field-aligned within a block. Further, each toroidal block can consist of a number of sub-blocks employed to represent a single-null poloidal cross-section as it is done in the 4D (axisymmetric) code. Assuming axisymmetric equilibrium magnetic geometry, the cell volumes can be constructed within each block in the same way. However, due to the twist and shear of the magnetic field lines the grids in different blocks will not, in general, be conformal. In order to provide communication between the blocks the grid in each block is extended (along the field lines) into the neighboring blocks, and such formed ghost-cells are filled by interpolating the corresponding valid-cell data. Due to the locally field-aligned nature of the discretization scheme the number of degrees of freedom to describe short-wavelength turbulence remains optimal. That is, while a 2D grid in the poloidal cross-section has to resolve fine-scale structures, e.g., $\lambda \sim \rho_i$, the toroidal direction, which plays the role of a field-aligned coordinate, can remain coarse as it only needs to resolve large-scale parallel structures. We note that some features of the discretization described here are conceptually similar to what is being used in Ref. [10] for the case of a finite-difference scheme applied to a 3D fluid model. The work in Ref. [10], however, considered the case of a flux-independent poloidal coordinate system. Here, we emphasize the use of a flux-aligned poloidal grid (with controlled dealignment in the X-point vicinity) in order to be consistent with the 4D transport version and to minimize numerical pollution from the electron physics effects (as described in Sec. 2). Finally, we comment on the use of the toroidal angle as a field-aligned coordinate (as employed here), in contrast to the poloidal angle, which is typically adopted for the modeling of core [11] and edge [12] turbulence. The choice of the poloidal angle as a field-aligned coordinate can be more efficient for modeling of high-n modes where it is sufficient to retain only a small part (wedge) of a full torus. Furthermore, it provides more natural specification of boundary conditions at the divertor plates. On the other hand, the use of the toroidal angle as a field-aligned coordinate is more natural for the X-point modeling where it yields minimal twist of control volumes.

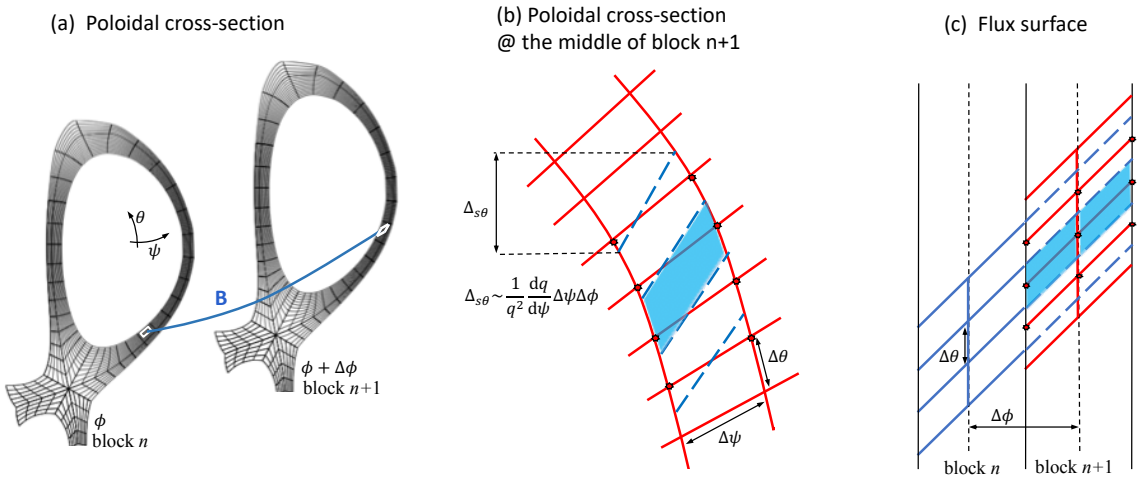

FIG. 3. Schematic of a locally field-aligned multiblock discretization scheme. Frame (a) shows poloidal cross-sections located in the middle of neighboring toroidal blocks. Assuming axisymmetric background magnetic geometry, the cross-sections are gridded in the same way. Note that the gridding is nearly flux-aligned and has poloidal sub-block structure to deal with the X-point. The control volumes for both valid and ghost cells are obtained in each block by mapping such poloidal grid along the magnetic field lines. A schematic twist and shift of a toroidal face mapped along a magnetic field-line is illustrated with two white parallelograms. Frame (b) shows the toroidal faces of block n ghost cells (the blue dashed lines) illustrated over the toroidal faces of block n+1 valid cells (the solid red lines). Frame (c) shows an example of the

toroidal block structure. In this case each block has two valid cells (shown with the solid blue and red lines) and two ghost cells. The location of the poloidal planes shown in Frame (a) corresponds to the vertical dashed lines in Frame (c). The shaded blue areas in Frames (b) and (c) illustrate the toroidal and radial faces of the same ghost cell, respectively. The star symbols in Frames (b) and (c) designate the three valid red cells that are used to evaluate the shaded blue ghost cell data for the case of a second-order interpolation.

Due to nonconformity of the toroidal cell faces at the shared block boundaries, special treatment of the intra-block interpolation and the evaluation of normal fluxes at the toroidal block boundaries is required to make a finite-volume scheme globally conservative. While development of a high-order conservative version of the proposed discretization is in progress, we have implemented a non-conservative second-order locally-field-aligned multiblock version of the code for the case of a sheared slab geometry, which can test critical aspects of the numerical scheme. This version utilizes a third-order upwind discretization of the gyrokinetic advection operator combined with a second-order interpolation scheme for the intra-block communication. The locally-aligned coordinate system is defined within each block as follows: the x (radial) coordinate labels the $y - z$ flux surface, the z (poloidal) coordinate designates the field-line as it crosses the $x - y$ (poloidal) plane in the middle of a block, finally the y (toroidal) coordinate measures the distance along a field line.

Here, we report on the first verification studies performed with the multiblock code for the test problem of the collisionless (universal) drift-wave instability (see Fig. 4). For this test the magnetic geometry is specified by $\boldsymbol{B} = B_0\boldsymbol{e_y} + (x/L_x)B_z\boldsymbol{e_z}$, where $B_0 = 3$ T, $B_z = 0.0008B_0$, and the domain extent is given by $L_x = L_z = 0.8$ cm, and $L_y = 10$ m. The ion and electron kinetic species are considered with $m_i = 2m_p$ and $m_e = 0.01m_p$, where m_p is the proton mass. The background distribution is assumed to be a Maxwellian plasma with an exponentially decaying density $L_n^{-1} = -n^{-1}\,dn/dx = 0.25L_x^{-1}$ and a uniform temperature $T_e = T_i = 400$ eV. The initial perturbations are taken as a first harmonic in the z and y directions, and a half-harmonic in the x direction. The simulation model solves the long wavelength limit of the full-F gyrokinetic equations for ion and electrons coupled to the gyroPoisson equation as described in detail in Ref. [4] reporting on verification of the single-block 5D version of the code. The boundary conditions are periodic in the z and y directions, and a zero-Dirichlet boundary condition is used for electrostatic potential perturbations at the radial (i.e., x) boundaries. The results of the multi-block locally field-aligned version of the COGENT code are found in agreement with the results obtained with the single-block slab version of the code, where the coordinate system corresponds to the (x, y, z) Cartesian coordinates. We note that a small value of the magnetic field pitch angle is chosen so that the Cartesian coordinates are nearly field-aligned, and therefore the single-block code can be used efficiently. It is also instructive to note that although the pitch angle is small the parallel wave vector varies by the factor of two across the radial (i.e., x) domain.

4. CONCLUSIONS

This work reports on the status of the gyrokinetic finite-volume code COGENT for edge plasma modelling. The concurrent progress is being made toward development of (a) an axisymmetric 4D code version for modeling of large-scale transport phenomena and (b) a full 5D version that includes small-scale turbulence. The present 4D version enables modelling of cross-separatrix transport time scale processes in realistic single-null geometries. The simulation model includes the nonlinear Fokker-Plank operator to describe ion-ion collisions, a self-consistent model for 2D potential variations and an ad-hoc model for anomalous radial transport. The 4D COGENT version has been tested in simulation of the DIII-D-like discharges (see Ref. [2] for details) and LTX-like discharges (see Sec. II). The development of the 5D code includes the 5D single-block Cartesian version as well as more advanced sheared-slab locally field-aligned multiblock version, which incorporates numerical algorithms designed to handle single-null geometries. Both versions have been successfully tested in the simulations of the collisionless drift-wave instability. Future work will include development of detailed electron and neutral models for the 4D transport version as well as extending the 5D code capabilities to support simulations in a single-null geometry.

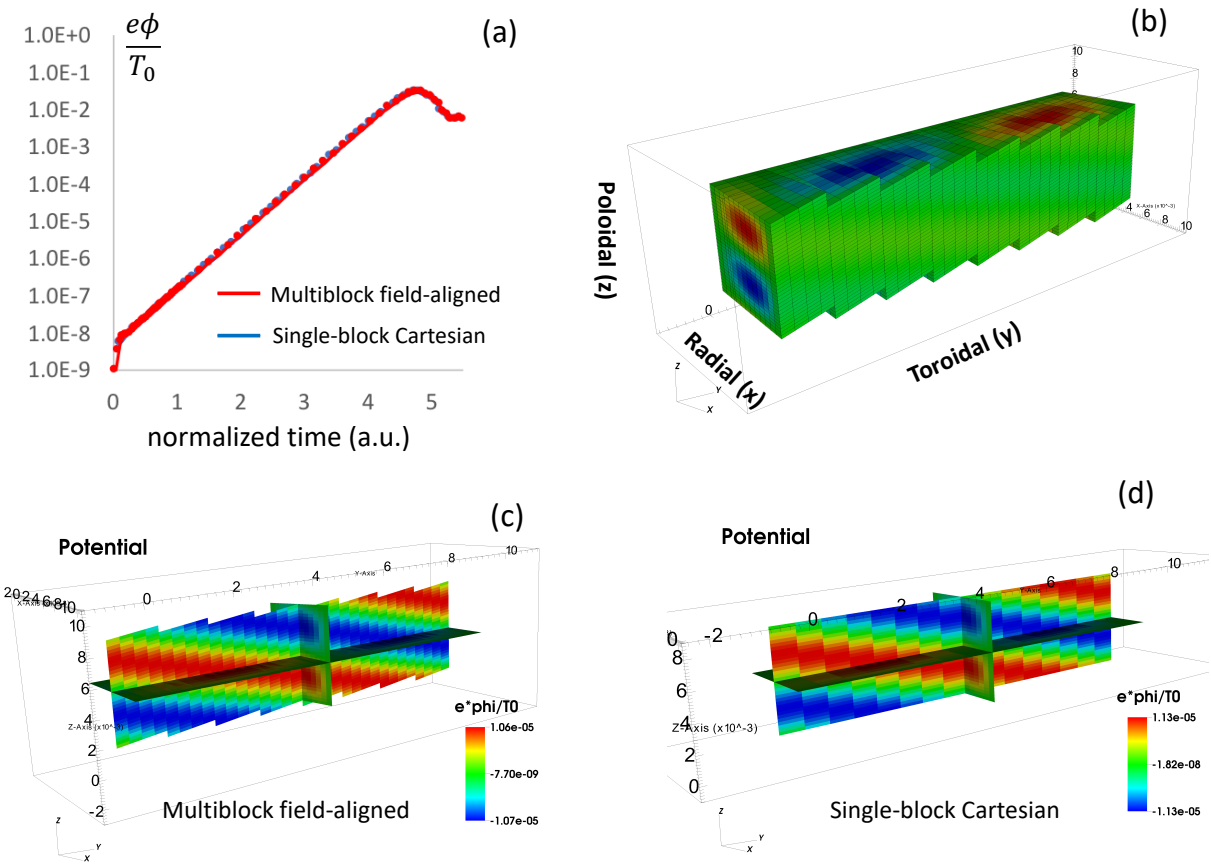

FIG. 4. 5D COGENT simulations of the collisionless drift-wave instability in a sheared-slab geometry performed with the single-block Cartesian version and the multiblock locally field-aligned version. Frame (a) shows excellent agreement in the time history of the maximum value of the potential perturbations. Frame (b) shows the multiblock structure: eight blocks are used with each block containing four field-aligned valid cells in the toroidal direction. The discretization also involves two ghost cells in each direction and on each side of a block (not shown). Frames (c) and (d) demonstrate the 3D structure of the potential perturbations for the multiblock and single-block cases, respectively. The grid resolution corresponds to $\left(N_x = 12, N_y = 32, N_z = 32, N_{v_\parallel} = 32, N_\mu = 16\right)$ *for the multiblock simulation and to* $\left(N_x = 12, N_y = 16, N_z = 32, N_{v_\parallel} = 32, N_\mu = 16\right)$ *for the single-block simulation.*

ACKNOWLEDGEMENTS

The authors are grateful to D. Majeski for fruitful discussions regarding details of the LTX experiment. They also wish to thank their collaborators in the Applied Numerical Algorithms Group, Lawrence Berkeley National Laboratory (LBNL), for their assistance in the development of the numerical algorithms and software infrastructure underlying the COGENT code. This research was supported by the U.S. Department of Energy under contract DE-AC52-07NA27344.

REFERENCES

[1] CHANG, C., KU, S., Spontaneous rotation sources in a quiescent tokamak edge plasma, Phys. Plasmas **15** (2008) 062510.

[2] DORF, M., DORR, M., Continuum kinetic modelling of cross-separatrix plasma transport in a tokamak edge including self-consistent electric fields, Contrib. Plasma Phys. **58** (2018) 434-444.

[3] DORF, M., et al., Progress with the COGENT Edge Kinetic Code: Implementing the Fokker-Planck Collision Operator, Contrib. Plasma Phys. **54** (2014) 517-523.
[4] LEE, W., et al., Verification of 5D continuum gyrokinetic code COGENT: Studies of kinetic drift wave instability, Contrib. Plasma Phys. **58** (2018) 445-450.
[5] DORR, M., et al., High-order discretization of a gyrokinetic Vlasov model in edge plasma geometry, J. Comp. Phys. **373** (2018) 605–630.
[6] ROZHANSKY, V., et al., Simulation of tokamak edge plasma including self-consistent electric fields, Nucl. Fusion **41** (2001) 387.
[7] ROGNLIEN, T., et al., Two-dimensional electric fields and drifts near the magnetic separatrix in divertor tokamaks, Phys. Plasmas **6** (1999) 1851.
[8] GHOSH, D., Kinetic simulation of collisional magnetized plasmas with semi-implicit time integration, J. Sci. Comput. (2018) https://doi.org/10.1007/s10915-018-0726-6.
[9] BOYLE, D., Observation of flat electron temperature profiles in the lithium tokamak experiment, Phys. Rev. Lett. **119** (2017) 015001.
[10] HARIRI, F., OTTAVIANI, M., A flux-coordinate independent field-aligned approach to plasma turbulence simulations, Comput. Phys. Commun. **184** (2013) 2419-2429.
[11] CANDY, J., WALTZ, R., An Eulerian gyrokinetic-Maxwell solver, J. Comput. Phys. **186** (2003) 545–581.
[12] UMANSKY, M., et al., Status and verification of edge plasma turbulence code BOUT, Comput. Phys. Commun. **180** (2009) 887-903.